Proceedings of the Institution of Mechanical Engineers, Part E: Journal of Process Mechanical Engineering

Experimental study of a hydrodynamic vortex separator

D A Egarr, M G Faram, T O'Doherty and N Syred

The online version of this article can be found at:
http://pie.sagepub.com/content/223/1/1

Published by:

$SAGE

http://www.sagepublications.com

On behalf of:

Institution of MECHANICAL ENGINEERS

Institution of Mechanical Engineers

Additional services and information for *Proceedings of the Institution of Mechanical Engineers, Part E: Journal of Process Mechanical Engineering* **can be found at:**

Email Alerts: http://pie.sagepub.com/cgi/alerts

Subscriptions: http://pie.sagepub.com/subscriptions

Reprints: http://www.sagepub.com/journalsReprints.nav

Permissions: http://www.sagepub.com/journalsPermissions.nav

Citations: http://pie.sagepub.com/content/223/1/1.refs.html

>> Version of Record - Feb 1, 2009

What is This?

Experimental study of a hydrodynamic vortex separator

D A Egarr[1], **M G Faram**[2], **T O'Doherty**[1*], and **N Syred**[1]

[1]Cardiff University, The Parade, Cardiff, UK

[2]Hydro International plc, Clevedon Hall Estate, North Somerset, UK

Abstract: A hydrodynamic vortex separator (HDVS) has been studied under laboratory conditions by using a specifically designed rig. Pressure tapping points placed at eight locations, six external and two internal, have revealed an even radial pressure distribution on the outer walls and central shaft. The ability of the HDVS to separate particulates has been studied. The particulates have been characterized by measurements of particle diameter and settling velocity, which have allowed efficiency cusps to be plotted against dimensionless groups used by other researchers. Owing to an unsatisfactory reduction of the data to a single curve by plotting the efficiency against dimensionless groups, an efficiency law has been determined based on the logistic equation and describes the separation efficiency in terms of the inlet flowrate, volume of the separator, and particle diameter and density.

Keywords: combined sewer overflow, hydrodynamic vortex separator, retention, separation, efficiency

1 INTRODUCTION

Older urban drainage systems, particularly in Europe, consist of combined sewers that are used to carry foul sewage and storm water. This can result in a large quantity of grit requiring removal at the preliminary stage of treatment, necessary to avoid damage to machinery such as pumps and valves, and accumulation in downstream process chambers [**1**]. One method of performing this is through the use of a hydrodynamic vortex separator (HDVS), whereby grit settles due to the force of gravity [**2**]. Sufficient residence time for this to take place is provided by the rotary nature of the path of the grit through the separator.

Figure 1 shows a schematic of a Grit King®, a form of HDVS analysed in this study, which is used for sewage grit removal [**3**]. The fluid enters the HDVS through a tangential inlet, marked in Fig. 1 by 'A', and upon entering the main chamber strikes a deflector plate 'B'. The fluid tends to take a path through the HDVS such that it rotates down around the outer part of the separator and upon reaching the bottom of the cone

'F' it rotates up through the central region between the dip plate 'E' and the central shaft 'G' before leaving through the overflow 'J'. Separated solids are collected in the grit pot 'H', which are removed either by an underflow component through the central underflow 'I' or by the use of a submersible pump, typically on an intermittent 'batch' basis. Hence, in this study, the HDVS is considered operating without an underflow component. The vent box 'C' allows the air trapped between the dip plate and the vessel wall 'D' to escape when the fluid level within the device fills the separator.

The operation of these systems to date has been difficult to quantify such that a single equation may be applied to predict the separation performance of such a device operating without an underflow. Many researchers have used dimensionless groups to reduce the spread of efficiency cusps, but few report on the successful fit of a function to the data. Frederick and Markland [**4**] related the efficiency to the dimensionless group $V_s C_d^{0.5}/U$, where V_s is the terminal settling velocity of the particle, C_d is the drag coefficient, and U is the mean velocity at the inlet. This was used while plotting retention efficiency curves for the particles entering a stilling pond – a form of combined sewer overflow (CSO) treatment chamber. This dimensionless group can be computed directly in combination with equation (1), when the particle

Corresponding author: School of Engineering, Cardiff University, The Parade, PO Box 925, Cardiff CF24 3AA, UK. email: odoherty@cf.ac.uk
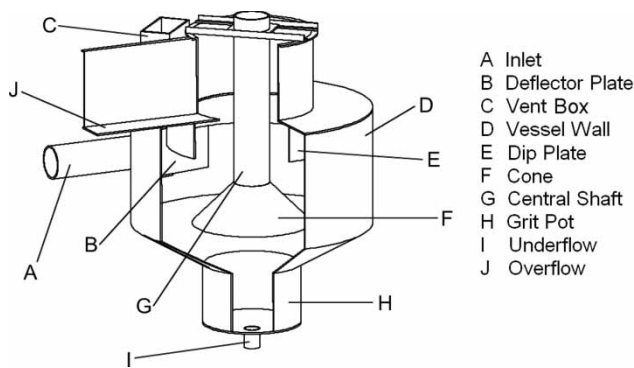
Fig. 1 Schematic of a 0.75 m diameter Grit King®

properties are known and the particles are assumed to be spherical

$$V_s = \sqrt{\frac{4dg(\rho_p - \rho_f)}{3C_d\rho_f}} \tag{1}$$

where d is the particle diameter, m; g is the acceleration due to gravity, m/s²; ρ_p is the particle density, kg/m³; and ρ_f is the fluid density, kg/m³.

Halliwell and Saul [5] by studying CSO chambers, related the efficiency to the dimensionless group V_s/U. Application of this group requires either knowledge of the particle settling velocity or knowledge of the particle properties such that the particle settling velocity may be computed theoretically [6].

Fenner and Tyack [7] proposed a 'hybrid' scaling law for particle retention efficiency that combined Froudian and Hazen scaling. The Froude number is given by $Q^2/D_S^5 g$, where D_S is the diameter of the HDVS, and the Hazen number, $(Q/A_S)/V_s$, where A_S is the plan area of the separator and Q is the inlet flowrate. A drawback of the scaling law proposed by Fenner and Tyack [7] is that the efficiency is calculated based on prior knowledge of the efficiency of a separator of a scaled size.

Researchers have found a relationship to describe the efficiency of an HDVS while operating with a constant underflow component [8]. This took the form of equation (2)

$$\eta = 1 - \left(1 - \frac{q}{Q}\right)\exp\left(-k\frac{V_s}{U}\right) \tag{2}$$

where q is the underflow discharge, m³/s, and k is a constant.

This function demonstrated that the efficiency was only dependent on the flow ratio q/Q and the ratio V_s/U. One limitation of this work was that it only considered particles of a single density.
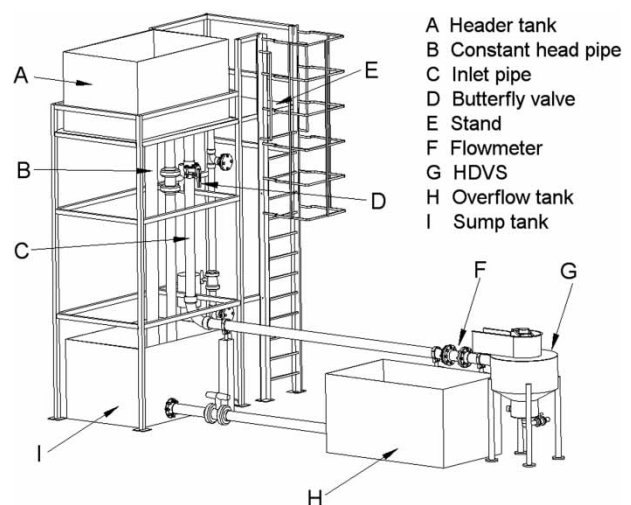
2 EXPERIMENTAL SETUP

Figure 2 shows a schematic of the custom-built rig used for testing the 0.75 m diameter HDVS.

Water is pumped to a header tank, marked 'A' in Fig. 2, where a constant head is maintained by the vertical pipe marked 'B'. Pipe 'C' is used for feeding water to the HDVS via a vertical section that comprises a butterfly valve 'D' chosen for ease of controlling the flow. A horizontal distance of ~45 diameters of straight pipe precedes the inlet to the separator so that a reasonably developed flow is allowed to establish. Particles are released into pipe 'C' in the header tank, where access can be gained by the stand 'E'. Release of the particles at this point was preferable to a stand pipe that would be positioned relatively close to the separator and would not allow a reasonable distance for the particles to settle before entering the separator, as it has been shown that the position of the particle at entry to an HDVS may affect the efficiency [9]. Hence, the particles enter the separator at what is thought to be a realistic position in the vertical plane of the inlet pipe. Flow measurement was via an electromagnetic flowmeter marked 'F'. Once water passes through the HDVS, marked 'G' in Fig. 2, it discharges into a tank 'H' connected to tank 'I' below the header tank. Hence, the flow circulates through the pumped system.

2.1 Retention efficiency testing

The particulate used for testing the HDVS included a pre-expanded polystyrene ('Styrocell') and an ion exchange resin used in water treatment applications ('Purolite'). Both types of particles are generally spherical, and hence, a sphericity of 1 can be assumed. The sphericity is defined as the surface area of a sphere with the same volume as the particle divided by the

Fig. 2 Schematic of the experimental rig used for testing the 0.75 m diameter HDVS

surface area of the particle [**6**], which is given by

$$\psi = \frac{4\pi(3V_\text{p}/4\pi)^{2/3}}{A_\text{p}} \tag{3}$$

where ψ is the sphericity, V_p is the volume of sphere, m^3, and A_p is the surface area of particle, m^2.

Although the density of the particles is supplied by the manufacturer/supplier of the particles, the figure is not exact. In the case of Styrocell, it is thought that pores of air may be trapped in the particle during the manufacturing process, which would explain why a fraction of particles float in water, despite the density being stated as being in the range 1020–1050 kg/m^3. Purolite expands when wet, and since it is an ion exchange resin, the density varies depending on what ions the particles have come into contact with. The particles were therefore characterized by taking dry samples that were sieved to reduce the size range. The volume of particles used in retention efficiency testing ranged from 100 to 900 ml, depending on the volume of particles available after sieving. Since Purolite expands when wet, it was left in water for approximately a week after sieving. Settling velocity tests were then carried out on a random sample of typically 50 individual particles in a sieved size range. The diameter of the settling column used was 0.25 m, and the maximum particle diameter can be assumed to be no more than 5.6 mm from the sieve sizes used. Hence, from a figure adapted from Fidleris and Whitmore [**10**], which accounts for wall effects on the terminal settling velocity of a particle, the diameter of the settling column is sufficient to neglect these. The temperature of the fluid was taken before and after the settling tests so that the density and viscosity of the water could be determined. Each settling test allowed the particle to settle in an adequate distance to allow the terminal settling velocity to be achieved. Using a stop watch, the particle would then be timed to fall a predetermined distance. The diameter of a random sample of typically 50 individual water soaked particles in a sieved size range was also measured by using Vernier callipers, taking care not to squash the particle while measuring its diameter. Ideally the diameter of all the particles in the sample used in the settling velocity tests would be taken, but due to the size of the particles, ease of handling did not allow this. Assuming the sphericity to be 1 and with the mean settling velocity and mean particle diameter known, as well as the fluid density and viscosity, a mean particle density can be calculated. This involves calculating the particle Reynolds number, equation (4), which is then used to calculate the drag coefficient from an equation proposed by Turton and Levenspiel [**11**]. The drag coefficient is then used in equation (1) to calculate the particle density. This has been done for all the particle sieve size ranges

used in retention efficiency testing

$$Re_\text{p} = \frac{dV_\text{s}\rho_\text{f}}{\mu} \tag{4}$$

where Re_p is the particle Reynolds number and μ is the absolute viscosity of fluid, kg/ms.

Faram *et al.* [**12**] have shown through experimentation that the efficiency of such devices is time-dependent since particles captured in the grit pot may be re-entrained into the flow. Each retention efficiency test was therefore carried out for 10 min, and the temperature of the fluid was taken at the start and end of each test. At the end of each test, the butterfly valve marked 'D', in Fig. 2, was closed before switching off the pump to prevent the particulates remaining in the HDVS from being flushed out by the water remaining in the header tank. The HDVS efficiency is defined by equation (5) and was determined by measuring the volume of particles, instead of measurement by mass, as this would include excess water held between the particles by surface tension. Drying the particles after each test would have been extremely time-consuming, particularly in the case of Purolite as each sample would have to be soaked for at least a week to allow the particles to expand

$$\eta = 100\frac{V_\text{GP}}{V_\text{T}} \tag{5}$$

where η is the efficiency, per cent, V_GP is the volume of particles remaining in the HDVS at the end of a test, and V_T is the volume of particles released into the system.

Comparisons of efficiency by using different volumes of particles have been made and it has been determined that the efficiency is independent of the particle loading for the volumes used in testing.

2.2 Pressure tapping measurements

The use of pressure tapping measurements to measure the static pressure at the walls has revealed an insight into the pressure distribution within the HDVS. BS EN ISO 5167 [**13**] outlines the guidelines for placing pressure tapping points on Venturi tubes, and wherever appropriate, these were applied in this study. Figure 3 shows the location of each pressure tapping point. Points 1–4 at the inlet were placed in a plane, i.e. 0.375 m from the centre-line of the HDVS and were arranged such that each was positioned 90° from each other on the circumference of the inlet pipe. Points 5–8 are located on the same plane as points 2 and 4 at the inlet. Points 9 and 10 on the central shaft are placed opposite points 5 and 7, respectively, and the static pressure on the outside of the shaft is measured. Points 11 and 12 are located half way down the grit pot, in the same plane as points 5 and 7.
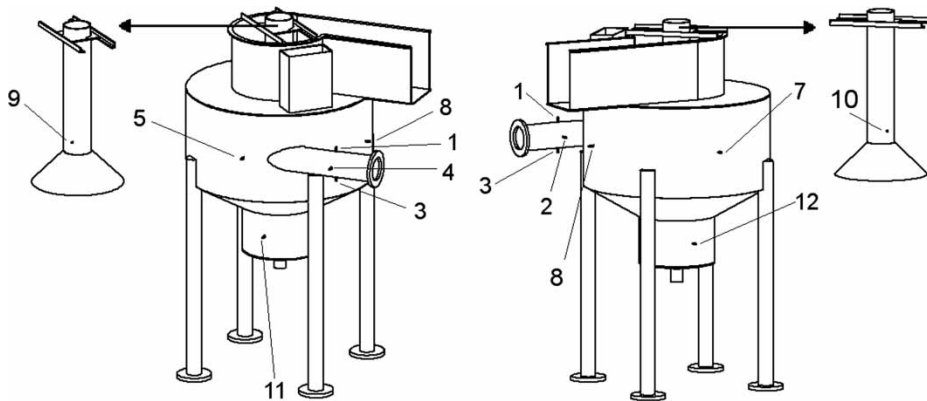
Fig. 3 Location of pressure tapping points on the 0.75 m diameter HDVS

3 RESULTS

3.1 Pressure tapping

An observation during the reading of the static pressure was that the fluctuations were very low, suggesting that the pressures at the walls are fairly stable. Three series of static pressure data were read from the four individual pressure tapping points at the inlet, which revealed negligible, if any, variation of the pressure around the circumference of the wall due to the length of the inlet pipe, which implied that a reasonably developed flow had been established. Figure 4 compares the static pressure readings taken in the HDVS. The data are the combined set of three series of readings and the repeatability of the data is consistent.

Points 5–8 are located around the central drum of the separator and the readings shown in Fig. 4 indicate that there is an equal pressure distribution around the outer circumference of the device, which is slightly higher than the pressure at the inlet. This could be

due to the reduced velocity of the fluid upon expansion from the inlet into the HDVS. The static pressure readings taken at points 9 and 10 are located on the central shaft, which is at the centre of the separator. Here, the static pressure is low compared with the pressure on the central drum of the separator, as would be expected from a vortex flow where the pressure increases radially outwards [14], and the rotation of the fluid creates a low-pressure axial core [15]. At points 11 and 12, situated on the grit pot, the static pressure is lower than at the inlet. This may be expected due to the diameter of the grit pot being less than the vessel. Hence, due to a pressure distribution, which increases radially outwards, the pressure at the wall of the main vessel would be expected to be higher than in the grit pot.

At flowrates of 3 l/s and lower, the pressure at each tapping point is almost identical. This implies that up to 3 l/s, the vortex flow is not fully developed due to the pressure on the central shaft and the vessel walls being identical.
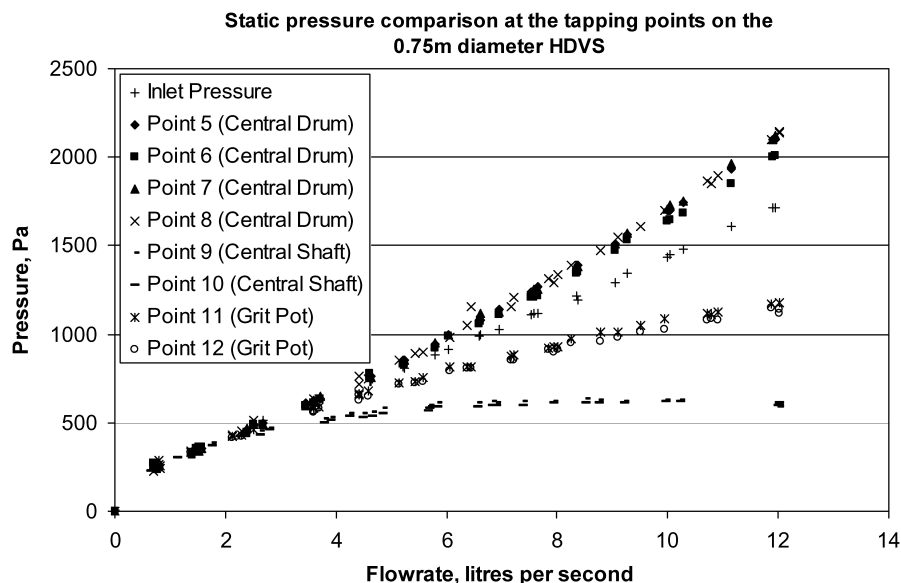

Fig. 4 Comparison of the static pressure readings in the 0.75 m diameter HDVS

3.2 Retention efficiency results

An observation during retention efficiency testing is that particles are drawn towards the centre of the separator. This would imply that the vortex generated within the HDVS tends more towards a free vortex than a forced one, where particles would be forced outside the device.

Plotting the retention efficiency against the inlet flowrate gives a series of efficiency cusps as shown in Fig. 5. Each efficiency cusp follows a definite trend and the repeatability of the data is consistent. The data for the Purolite 500–710 μm sieve range were not repeated due to the time required to collect all the particulate. Efficiencies for Styrocell 1.4–2.0 mm below 4.25 l/s cannot be achieved because at lower flowrates, the particles tend to flocculate and begin to float. At higher flowrates, the turbulence in the flow prevents the flocs forming. Flowrates >12 l/s cannot currently be achieved due to facility constraints. Initially, the trend in the efficiency cusps appears to be with settling velocity of the particles, but upon closer inspection it can be seen that the particles, Purolite 500–600 μm, have the highest efficiency despite having a settling velocity lower than Styrocell 2.8–5.6 mm, as detailed in Table 1.

Figure 6 shows the efficiency as a function of $Q^2/D_S^5 g$ (Froude number), $V_s C_d^{0.5}/U$, and V_s/U.

From Fig. 6, where the efficiency has been plotted as a function of the Froude number, it may be implied that the ratio of the inertia to gravity forces in the separator has negligible effect on the efficiency due to the lack in reduction of the spread of data. This result has also been observed by Luyckx *et al.* [**8**] who studied an HDVS operating with a constant underflow. The dimensionless group $V_s C_d^{0.5}/U$ brings the curves closer together, implying that the particle properties have

Table 1 Particle properties

Particle type and sieve size range	Mean settling velocity (m/s)	Mean settling velocity standard deviation (%)	Mean particle surface load (kg/m²)
Purolite 500–600 μm	0.026 27	6.9	0.2112
Styrocell 2.8–5.6 mm	0.034 29	9.1	0.1009
Styrocell 2.0–2.8 mm	0.029 25	11.7	0.0843
Styrocell 1.4–2.0 mm	0.020 87	6.9	0.0625
Purolite 710–1000 μm	0.009 66	9.8	0.0408
Purolite 500–710 μm	0.006 86	13.3	0.0350

a greater impact on the efficiency. When the efficiency is expressed as a function of V_s/U, the efficiency cusps are brought closer together again suggesting that the efficiency is more strongly linked with the settling velocity of the particle.

Although the data have been brought closer together while plotting V_s/U, at a value of V_s/U equal to ∼0.4 a variation in efficiency of ∼50 per cent exists, where the efficiency of Styrocell 2.8–5.6 mm is ∼30 per cent and the efficiency of Purolite 500–600 μm is ∼80 per cent. Hence, a satisfactory single curve has not been achieved.

Figure 5 shows a series of curves that are in the form of a backward 'S'. Plotting efficiency as a function of V/Q, where V is the volume of fluid in the separator and Q is the inlet flowrate, inverts the 'S' curve and also takes into account the size of the separator. An 'S' curve may be described by the logistic function, as in equation (6), which was developed for modelling population growth [**16, 17**]

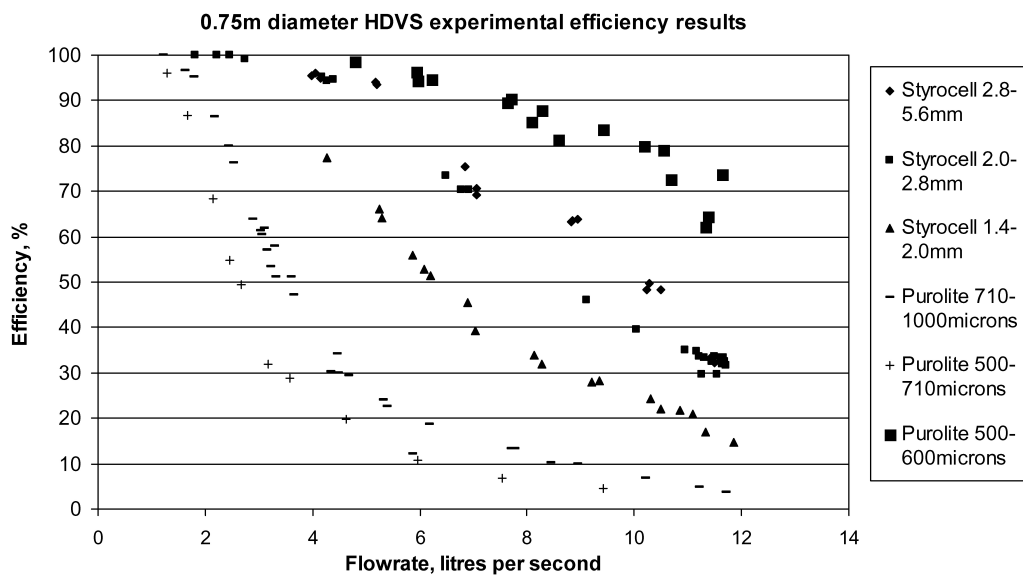$$f(x) = A \frac{1 + Be^{-Cx}}{1 + De^{-Cx}} \qquad (6)$$

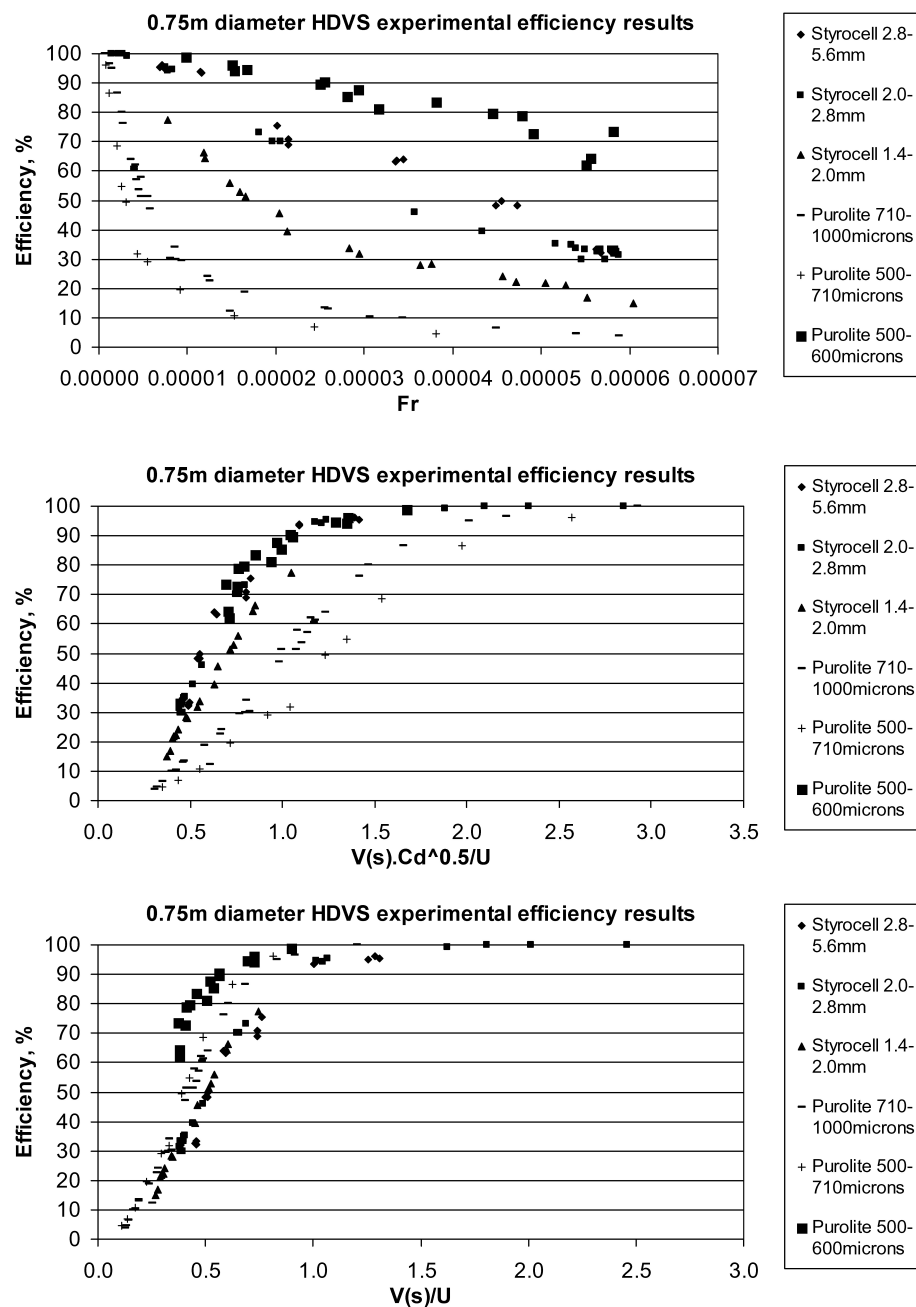**Fig. 5** Efficiency versus flowrate for the 0.75 m diameter HDVS

Fig. 6   HDVS efficiency as a function of various dimensionless groups

Equation (6) is a four-parameter model, i.e. it requires four constants to be specified; but by examination of the function, this may be reduced. First, the term Be^{-Cx} applies negative growth in that when $B \to D$ the function approaches a straight line; therefore $B = 0$. Now, when $x \to \infty, f(x) \to A$. Obviously, $A = 100$ as the efficiency does not exceed 100 per cent. The function can now be written as

$$\eta = \frac{100}{1 + De^{-Cx}} \qquad (7)$$

Equation (7) is a two-parameter model. The coefficients that give the best fit in a two-parameter model may be determined by using an optimization

technique by Guymer [**18**]. This involves determining the R_t^2 value [**19**] for a matrix of values of C and D, and reducing the range between the constants that give the highest R_t^2 value until a satisfactory accuracy has been achieved for each. This has been done for each efficiency cusp, when plotted against V/Q.

By plotting various quantities for the full range of particles used, it has been found that the quantity that appears to be controlling the efficiency is mass diffusion, which is given by

$$m_d = d(\rho_p - \rho_f) \qquad (8)$$

where m_d is the particle surface load, kg/m^2.

Table 1 lists the average particle settling velocity, the standard deviation of the settling velocity expressed as a percentage of the mean, and also particle surface load based on the mean particle diameter and density.

Hence, the larger the mass diffusion the higher the expected efficiency. Thus, by plotting C and D in the logistic equation against the mass diffusion, it can be seen that a function exists as illustrated in Fig. 7. (These constants have been normalized only for the purpose of publication.) In Fig. 7, those points that have been circled are 'dummy' points, used to aid fitting a trend line and are justified in that they

aid the function to consistently predict the efficiency cusps that increase when the mass diffusion increases, as observed with the experimental data. The functions that best describe the relationship between C and D are polynomials. Hence, the efficiency of the 0.75 m diameter HDVS may be predicted for any particle with a mass diffusion in the range for which experimental testing has been carried out. The model is thus dependent on the inlet flowrate, which is the same as the overflow flowrate, the volume of fluid within the separator, and the particle density and diameter. Figure 8 shows a good fit by the model to a range of efficiency cusps.
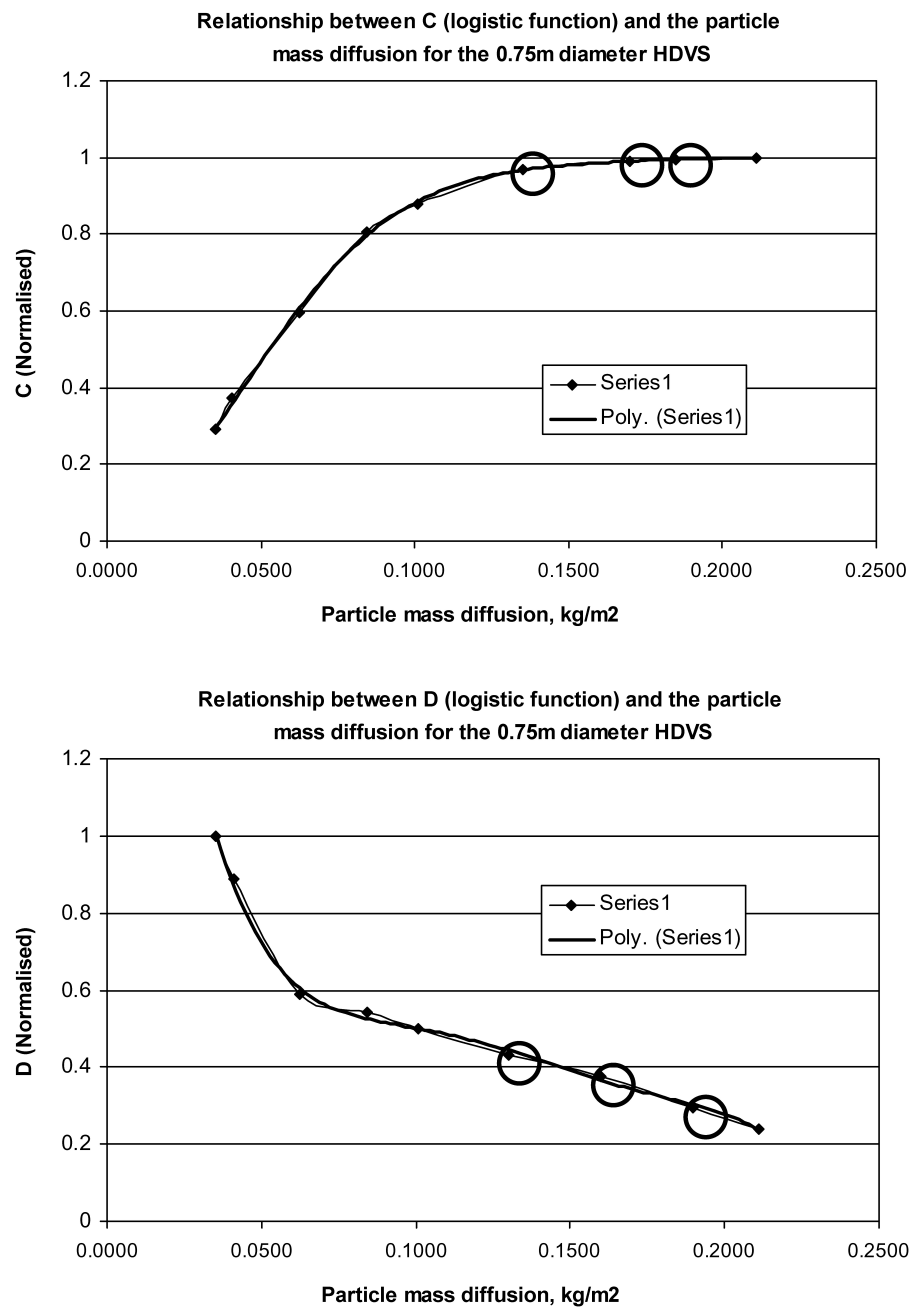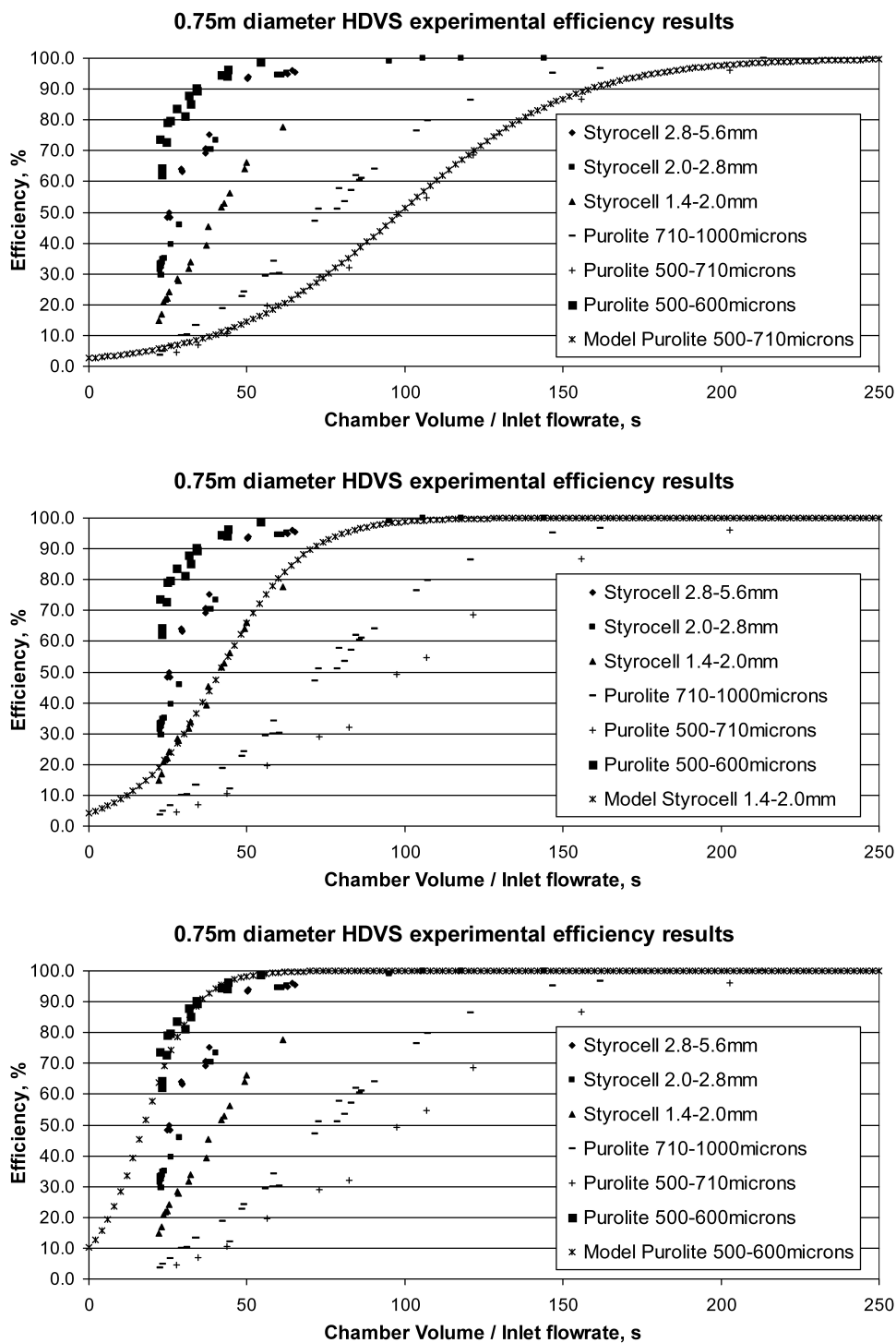

Fig. 7 Relationship between C and D in the logistic function and the particle surface load

0.75m diameter HDVS experimental efficiency results

0.75m diameter HDVS experimental efficiency results

0.75m diameter HDVS experimental efficiency results

Fig. 8 Comparison of the model and experimental retention efficiency results for the 0.75 m diameter HDVS

4 DISCUSSION

An experimental study has been carried out to investigate the operational and performance attributes of an HDVS by using a custom-built rig to attain accurate separation efficiencies of particulates. Pressure tapping data have revealed an even radial pressure distribution on the outer walls and central shaft, and it is observed that the vortex flow within the HDVS is not fully developed at a flowrate <3 l/s in this particular size of separator. Particulates have been characterized using measurements of particle diameter and terminal settling velocity, which has allowed the mean particle density to be calculated rather than relying on manufacturers specifications. Plotting retention efficiency as a function of dimensionless groups, used

by previous researchers, has not resulted in a satisfactory single-efficiency cusp. The efficiency has therefore been defined by the logistic function, where the constants are described as a function of the particle surface load. A limitation of the model is that the predicted efficiency is never 0 per cent as the logistic equation in the form of equation (7) is asymptotic to $y = 0$. However, the offset is fairly small and when sizing a separator the required efficiency tends to be of the order of 95 per cent, where it can be seen that the model gives an adequate prediction. The functions that best fit the constants in the logistic equation are polynomials. This means that the model is only valid for particles with a mass diffusion within the range used in testing. Further work is required to attain a more complete relationship for the constants. The model does not take into account the shape factor of the particle, since it is assumed that the particles used in testing are spherical. The viscosity of the fluid is also not taken into account, depending on the nature and concentration of 'contaminants' in the water and its temperature. Although the model does consider the size of the HDVS in that it takes into account the volume of fluid in the separator, the application of the model to HDVSs larger or smaller than 0.75 m has to be validated.

A possible limitation of the testing is that the results are for a specific test period, and therefore does not account for particle re-entrainment that could occur over a longer duration. However, HDVSs of the investigated form have been demonstrated by others to be relatively resistant to this phenomenon compared to other devices with 'exposed' particle collection regions [**12**]. A straight pipe of 45 diameters upstream of the inlet may be unlikely, where these systems are installed in practice. However, efficiency predictions with a developed velocity profile at the inlet to the HDVS are a basis for comparisons with different configurations of upstream pipe work. The method behind the derivation of the efficiency model is a building block for further studies on large scale HDVSs.

5   CONCLUSIONS

1. The pressure distribution within an HDVS has found to be an even radial distribution on the walls and the central shaft where the vortex flow becomes developed at a flowrate of 3 l/s.
2. Retention efficiency has been plotted as a function of dimensionless groups used by previous researchers, none of which has reduced the efficiency to a single cusp.
3. Retention efficiency testing has revealed that efficiency cusps are dependent on particle surface load and not particle settling velocity.
4. A model for predicting the efficiency of an HDVS has been developed by using the logistic equation.

REFERENCES

1 Gardner, P. and **Deamer, A.** An evaluation of methods for assessing the removal efficiency of a grit separation device. *Water Sci. Technol.*, 1996, **33**(9), 269–275.
2 Andoh, R. Y. G. and **Smisson, R. P. M.** High rate sedimentation in hydrodynamic separators. In 2nd International Conference on Hydraulic Modelling Developmentand Application of Physical and Mathematical Models, Stratford, UK, 14–16 June 1994, pp. 341–358.
3 Faram, M. G., James, M. D., and **Williams, C. A.** Wastewater treatment using hydrodynamic vortex separators. In CIWEM/AETT 2nd National Conference, Wakefield, UK, 13–15 September 2004, pp. 79–87.
4 Frederick, M. R. and **Markland, E.** The performance of stilling ponds in handling solids. Paper 5: ICE Symposium on Storm Sewage Overflows, London, UK, 1967, pp. 51–61.
5 Halliwell, A. R. and **Saul, J.** The use of hydraulic models to examine the performance of storm-sewage overflows. *Proc. Inst. Civ. Eng., Part 2*, 1980, **69**, 245–259.
6 Brown, N. P. and **Heywood, N. I.** *Slurry handling design of solid–liquid systems*, 1991 (Elsevier Science Publishers Ltd, England).
7 Fenner, R. A. and **Tyack, J. N.** Scaling laws for hydrodynamic separators. *J. Environ. Eng.*, 1997, **123**(10), 1019–1025.
8 Luyckx, G., Vaes, G., and **Berlamont, J.** Experimental investigation on the efficiency of a hydrodynamic vortex separator. In 3rd International Conference on Innovative Technologies in Urban Storm Drainage, Novatech, Lyon, France, 4–6 May 1998, pp. 443–450.
9 Egarr, D. A., Faram, M. G., O'Doherty, T., and **Syred, N.** An investigation into the factors that determine the efficiency of a hydrodynamic vortex separator. In 5th International Conference, Sustainable Techniques and Strategies in Urban Water Management, Novatech, Lyon, France, 7–11 June 2004, pp. 61–68 (ISBN 2-9509337-5-0).
10 Fidleris, V. and **Whitmore, R. L.** Experimental determination of the wall effect for spheres falling axially in cylindrical vessels. *Br. J. Appl. Phys.*, 1961, **12**, 490–494.
11 Turton, R. and **Levenspiel, O.** A short note on the drag correlation for spheres. *Powder Technol.*, 1986, **47**, 83–86.
12 Faram, M. G., Harwood, R., and **Deahl, P. J. D.** Investigation into the sediment removal and retention capabilities of stormwater treatment chambers. In StormCon Conference, San Antonio, Texas, 28–31 July 2003.
13 British Standards Institution, BS-EN-ISO 5167-1:2003. Measurement of fluid flow by means of pressure differential devices – part 1: orifice plates, nozzles, and Venturi tubes inserted in circular cross-section conduits running full, 2003.

14 Svarovsky, L. *Hydrocyclones*, 1984 (Rinehart and Winston Ltd, East Sussex, England).

15 Bradley, D. *The hydrocyclone*, 1st edition, 1965 (Pergamon Press, Great Britain).

16 Verhulst, P.-F. Recherches mathématiques sur la loi d'accroissement de la population. *Nouv. mém. de l'Academie Royale des Sci. et Belles-Lettres de Bruxelles*, 1845, **18**, 1–41.

17 Verhulst, P.-F. Deuxième mémoire sur la loi d'accroissement de la population. *Mém. de l'Academie Royale des Sci., des Lettres et des Beaux-Arts de Belgique*, 1847, **20**, 1–32.

18 Guymer, I. A national database of travel time, dispersion and methodologies for the protection of river abstractions. Environment Agency R & D Technical Report, 2002 (ISBN 1 85705 821 6).

19 Young, P., Jakeman, A., and **McMurtrie, R.** An instrument variable method for model order identification. *Automatica*, 1980, **16**, 281–294.

APPENDIX

Notation

A	constant (dimensionless)
A_p	surface area of particle (m²)
A_S	plan area of the HDVS (m²)
B	constant (dimensionless)
C	constant (dimensionless)
C_d	drag coefficient (dimensionless)
d	particle diameter (m)
D	constant (dimensionless)
D_S	diameter of the HDVS (m)
g	acceleration due to gravity (m/s²)
k	constant (dimensionless)
m_d	particle surface load (kg/m²)
q	underflow discharge (m³/s)
Q	inlet flowrate (m³/s)
Re_p	particle Reynolds number (dimensionless)
U	mean velocity at the inlet (m/s)
V	volume of fluid (m³)
V_{GP}	volume of particles remaining in the HDVS at the end of a test (m³)
V_p	volume of sphere (m³)
V_s	particle terminal settling velocity (m/s)
V_T	volume of particles released into the system (m³)
η	efficiency (per cent)
μ	absolute viscosity of fluid (kg/ms)
ρ_f	fluid density (kg/m³)
ρ_p	particle density (kg/m³)
ψ	sphericity (dimensionless)